frontiers in
GENETICS

ORIGINAL RESEARCH ARTICLE
published: 08 August 2012
doi: 10.3389/fgene.2012.00138

Increased expression of rififylin in $a < 330$ kb congenic strain is linked to impaired endosomal recycling in proximal tubules

Kathirvel Gopalakrishnan[1,2], Sivarajan Kumarasamy[1,2], Yanling Yan[3,4], Jiang Liu[3], Andrea Kalinoski[5,6], Anbarasi Kothandapani[7], Phyllis Farms[1,2] and Bina Joe[1,2]*

[1] Center for Hypertension and Personalized Medicine, University of Toledo College of Medicine and Life Sciences, Toledo, OH, USA
[2] Department of Physiology and Pharmacology, University of Toledo College of Medicine and Life Sciences, Toledo, OH, USA
[3] Department of Medicine, University of Toledo College of Medicine and Life Sciences, Toledo, OH, USA
[4] Institute of Biomedical Engineering, Yanshan University, Qinhuangdao, China
[5] Department of Surgery, University of Toledo College of Medicine and Life Sciences, Toledo, OH, USA
[6] Advanced Microscopy Imaging Center, University of Toledo College of Medicine and Life Sciences, Toledo, OH, USA
[7] Department of Biochemistry and Cancer Biology, University of Toledo College of Medicine and Life Sciences, Toledo, OH, USA

Edited by:
Howard Prentice, Florida Atlantic University, USA

Reviewed by:
Akihiro Ikeda, University of Wisconsin Madison, USA
Howard Prentice, Florida Atlantic University, USA

***Correspondence:**
Bina Joe, Department of Physiology and Pharmacology, Center for Hypertension and Personalized Medicine, University of Toledo College of Medicine and Life Sciences, 312, Block Health Science Building, 3000 Transverse Dr., Toledo, OH 43614, USA.
e-mail: bina.joe@utoledo.edu

Cell surface proteins are internalized into the cell through endocytosis and either degraded within lysosomes or recycled back to the plasma membrane. While perturbations in endosomal internalization are known to modulate renal function, it is not known whether similar alterations in recycling affect renal function. Rififylin is a known regulator of endocytic recycling with E3 ubiquitin protein ligase activity. In this study, using two genetically similar strains, the Dahl Salt-sensitive rat and an S.LEW congenic strain, which had allelic variants within $a < 330$ kb segment containing rififylin, we tested the hypothesis that alterations in endosomal recycling affect renal function. The congenic strain had 1.59-fold higher renal expression of rififylin. Transcriptome analysis indicated that components of both endocytosis and recycling were upregulated in the congenic strain. Transcription of *Atp1a1* and cell surface content of the protein product of *Atp1a1*, the alpha subunit of Na^+K^+ATPase were increased in the proximal tubules from the congenic strain. Because rififylin does not directly regulate endocytosis and it is also a differentially expressed gene within the congenic segment, we reasoned that the observed alterations in the transcriptome of the congenic strain constitute a feedback response to the primary functional alteration of recycling caused by rififylin. To test this, recycling of transferrin was studied in isolated proximal tubules. Recycling was significantly delayed within isolated proximal tubules of the congenic strain, which also had a higher level of polyubiquitinated proteins and proteinuria compared with S. These data provide evidence to suggest that delayed endosomal recycling caused by excess of rififylin indirectly affects endocytosis, enhances intracellular protein polyubiquitination and contributes to proteinuria.

Keywords: carp-2, kidney disease, hypertension, rat, linkage mapping, gene, rffl, proteinuria

INTRODUCTION

The composition of plasma membranes of virtually all eukaryotic cells is established, maintained, and remodeled by exocytosis, endocytosis, and a process of membrane recycling facilitated by endosomes. Cells are estimated to internalize their cell surface equivalent one to five times per hour (Steinman et al., 1983). This rapid removal of membrane from the cell surface is balanced by endosomal recycling pathways, which return most of the endocytosed proteins and lipids back to the plasma membrane (Maxfield and McGraw, 2004). Thus, a stringent regulation of recycling is essential to maintain the balance between endocytic uptake and recycling pathways. Disruptions in endocytosis and recycling are known to adversely affect diverse cellular processes (Yamamoto et al., 2000; Hryciw et al., 2006; Golachowska et al., 2010; Stendel et al., 2010).

Kidneys reabsorb >95% of all proteins filtered through the glomerular apparatus (Nielsen, 1993). Proteinuria is one of the markers of renal dysfunction. Within the apical membranes of proximal tubule cells in the kidney, an extensive endocytic apparatus plays a key role in the reabsorption and degradation of glomerular-filtered albumin and other proteins (Marshansky et al., 2002) and in the recycling of many functionally important membrane transporters (Brown and Stow, 1996). We hypothesized that any alterations in endosomal recycling disrupts cellular homeostasis and thereby could affect renal function. The current study was designed to test whether altered endosomal recycling facilitated by a congenic segment previously mapped on rat chromosome 10 containing rififylin (Gopalakrishnan et al., 2011) can affect renal molecular and cellular physiology and thereby contribute to the extent of

protein excretion in a rat model of cardiovascular and renal disease.

MATERIALS AND METHODS

ANIMALS

All of the animal experiments were conducted in accordance with the National Institutes of Health Guide for the Care and Use of Laboratory Animals and as per approved protocols by the institutional animal care and use review committee of the University of Toledo College of Medicine and Life Sciences. The congenic strain used in the current study was constructed in our laboratory using S and LEW rats. The strain is designated as S.LEW (10) × 12 × 2 × 3 × 5 and the construction of this congenic strain is detailed elsewhere (Gopalakrishnan et al., 2011).

cDNA ANALYSES

mRNA from kidneys of neonates and 53 days old rats were extracted using TRIzol Reagent (Life Technologies). cDNA was obtained by reverse transcription with SuperScript III (Invitrogen) using an Oligo dT primer. Using genomic sequence data for rat *Rffl* gene available at the Ensembl website[1], sense (5′CAGCTGAAGGAGATCCTGGC3′) and antisense (5′CCATGCAAATCTTACACAGGTTC3′) primers were designed to amplify exons 4–6 of the *Rffl* transcript by PCR. The resultant cDNA product was confirmed by sequencing using services provided by MWG Biotech Inc. DNA alignments were done using the sequence analysis software *Sequencher* from GeneCodes Corporation. Transcript expression of *Rffl* was analyzed by Real-Time PCR (BioRad) and expression levels relative to *Gapdh* were calculated by the $2^{-\Delta\Delta CT}$ method (Livak and Schmittgen, 2001).

IMMUNOBLOT ANALYSES

Protein lysates were prepared as described previously (Gopalakrishnan et al., 2011) and subjected to Tricine/SDS-PAGE, transferred to PVDF membrane, incubated with specific primary antibodies followed by secondary antibodies and processed by ECL. Membranes were re-probed with monoclonal anti-Gapdh. The immunoblots were analyzed by densitometric scanning using Image J software. Sources of primary antibodies: Cell Signaling Technology (anti-Gapdh), Abcam (anti-Rffl), the Developmental studies hybridoma bank at the University of Iowa (monoclonal antibody against the Na^+K^+ATPase α-1 subunit, clone α6F), Santa Cruz Biotechnology (Donkey anti-rabbit IgG-HRP conjugate).

EARLY ENDOSOME ISOLATION AND WESTERN BLOT ANALYSIS OF NA^+K^+ATPASE α1 SUBUNIT

Early endosome (EE) fractions (Eea-1 and Rab5 positive) were isolated from renal proximal tubules by sucrose flotation centrifugation as previously described (Liu et al., 2011). The enrichment of EE fractions was assessed by the EE marker Eea-1. Equal amount of total proteins (25 μg) from the EE fraction of each sample was precipitated with trichloroacetic acid for subsequent western blot analysis.

[1]www.ensembl.org

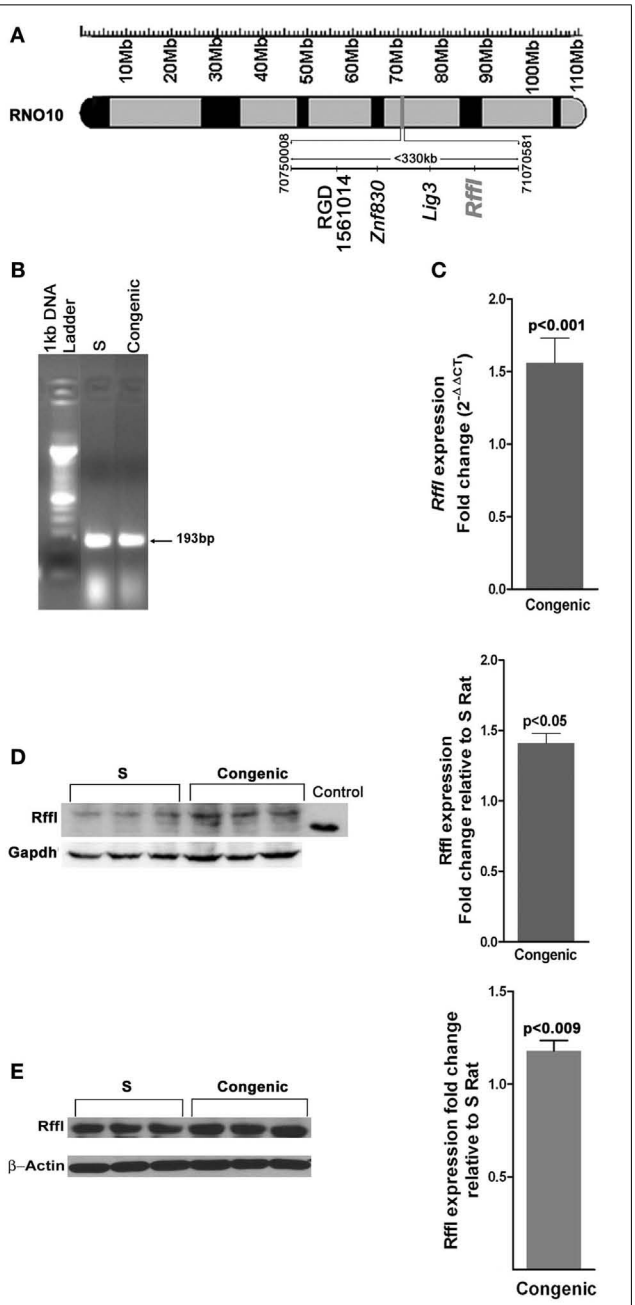

FIGURE 1 | (A) Schematic diagram of the congenic strain used in the study. The <330 kb region spanned by the congenic strain S.LEW (10) × 12 × 2 × 3 × 5 is shown alongside the physical map of rat chromosome 10. The basepairs delineating the ends of the congenic segment and the gene annotations were obtained from Ensembl.org. (RGSC 3.4) RNO10, Rat chromosome 10; Mb, Megabases. **(B)** Expression of *Rffl* transcript in the kidneys at 53 days of age as detected by RT-PCR. **(C)** Quantification of *Rffl* transcripts relative to S rats by real-time PCR using whole kidney samples from 53-day-old rats ($n = 6$ animals per group). Immunoblot of Rffl in **(D)** whole-cell lysates from S ($n = 3$) and congenic ($n = 3$) rat kidneys at 53 days of age; **(E)** proximal tubules from S ($n = 3$) and congenic ($n = 3$). RFFL (NP_0010717368, 2aa-99aa, 36.41 kDa) partial recombinant protein was used as positive control and Gapdh was the loading control. Quantification of Rffl protein ± SEM is shown alongside.

Table 1 | Differentially expressed transcripts in the clathrin-mediated endocytosis network.

Affymetrix ID	Fold change	*p*-Value	Symbol	Entrez gene name
1369733_at	2.201	0.0258	*Ctnnb1*	Catenin (cadherin-associated protein), beta 1, 88 kDa
1393288_at	1.897	0.0366	*Rab5b*	RAB5B, member RAS oncogene family
1398825_at	1.802	0.0434	*Rab11b*	RAB11B, member RAS oncogene family
1371113_a_at	1.787	0.0411	*Tfrc*	Transferrin receptor (p90, CD71)
1368762_at	1.749	0.0232	*Ubd*	Ubiquitin D
1399153_at	1.715	0.0356	*Rab5b*	RAB5B, member RAS oncogene family
1369998_at	1.708	0.0268	*Arf6*	ADP-ribosylation factor 6
1372513_at	1.63	0.0268	*Rac1*	Ras-related C3 botulinum toxin substrate 1
1388022_a_at	1.459	0.018	*Dnm1l*	Dynamin 1-like
1388104_at	1.436	0.0225	*Igr4*	Leucine-rich repeat containing G protein-coupled receptor 4
1370672_a_at	1.416	0.0422	*Dnm3*	Dynamin 3
1374232_at	1.416	0.0166	*Pik3ca*	Phosphoinositide-3-kinase, catalytic, alpha polypeptide
1384101_at	1.414	0.0362	*Wasl*	Wiskott–Aldrich syndrome-like
1370081_a_at	1.409	0.0236	*Vegfa*	Vascular endothelial growth factor A
1384750_at	1.392	0.037	*Numb*	Numb homolog (*Drosophila*)
1395548_at	1.378	0.0331	*Eps15*	Epidermal growth factor receptor pathway substrate 15
1392643_at	1.355	0.0355	*Rab5b*	RAB5B, member RAS oncogene family
1387170_at	1.238	0.0473	*Csnk2a1*	Casein kinase 2, alpha 1 polypeptide
1368096_at	-1.291	0.0321	*Rab7l1*	RAB7, member RAS oncogene family like 1

Statistical analyses of the microarray data were performed with RMA, robust multiarray averaging; BH, Benjamini and Hochberg adjustment using the R statistical package (version 2.8.1). The complete microarray data is available to the reviewers at the following link: http://www.ncbi.nlm.nih.gov/geo/query/acc.cgi?token=hryjdweamuioidi&acc=GSE30770

WHOLE GENOME TRANSCRIPTIONAL PROFILING

RNA was isolated from the kidneys of concomitantly raised, male, 53-day-old S, and congenic rats ($n = 6$ per group) using TRIzol and purified by RNeasy kit (Qiagen). RNA from two animals was pooled. Three such pooled RNA samples from S and congenic rats were hybridized to Affymetrix Rat Expression Arrays 230 2.0. The arrays were scanned at the Genomics core laboratory of the University of Toledo http://www.utoledo.edu/med/depts/bioinfo/cores/genointro.html. Statistical analyses of the microarray data were performed using the R statistical package (version 2.8.1). The microarray data are in compliance with the Minimum Information About Microarray Experiments and were uploaded into the Gene Expression Omnibus database[2]. Pathway analysis was conducted using Ingenuity Systems Pathway Analysis[3].

ISOLATION AND PRIMARY CULTURE OF RAT PROXIMAL TUBULE CELLS

Primary rat proximal tubule (RPT) cells were isolated from cortices of rat kidneys from S and congenic rats as described previously (Liu et al., 2011).

LABELING OF CELL SURFACE NA/K-ATPASE BY BIOTINYLATION

Cell surface biotinylation of Na/K-ATPase in proximal tubule primary cultures was performed as previously described (Liu et al., 2002, 2004, 2011). After surface biotinylation with EZ-Link sulfo-NHS-ss-Biotin (Pierce) and immobilization with ImmunoPure immobilized streptavidin-agarose beads (Pierce), biotinylated proteins were eluted after incubation in a 55°C water bath for 30 min, mixed with an equal volume of 2× Laemmli sample buffer, resolved by 10% SDS-PAGE, and then immunoblotted.

TRANSFERRIN RECYCLING

Transferrin recycling was studied as described previously (Gopalakrishnan et al., 2011). In brief, isolated proximal tubules were maintained at 37°C with 5% CO_2 and allowed to internalize a fluorescent derivative of transferrin (Alexa^{488}-Tf, Molecular Probes) for 90 min at 37°C and washed three times with ice cold PBS. Recycling was induced by warming the cells to 37°C in a serum free medium containing 0.1% BSA and a 100-fold excess of unlabelled holotransferrin (Sigma) and monitored by live imaging using a Leica TCS SP5 laser scanning confocal microscope. Just before monitoring, DRAQ5 was added to visualize the nuclei. Cells were imaged using a 488 and 433 laser line in the *XY* plane with scanning set at 30 s intervals for 30 min. Paired time lapse studies were performed in triplicate using the same gain, offset, and laser power settings to ensure that there were no intensity differences due to the acquisition settings between S and Congenic. Mean fluorescent intensity was measured in Image J at individual time points of the acquired images.

POLYUBIQUITINATED PROTEINS

Polyubiquitin-modified proteins were isolated from kidneys using the Pierce Ubiquitin Enrichment Kit as per previously published procedures (Gopalakrishnan et al., 2011).

[2]http://www.ncbi.nlm.nih.gov/geo/query/acc.cgi?token=hryjdweamuioidi&acc=GSE30770

[3]www.ingenuity.com

URINARY PROTEIN EXCRETION

Urinary Protein Excretion (UPE) determination was done as previously described (Kumarasamy et al., 2011). Briefly, at 53 days of age, rats fed with low salt (0.3% NaCl) was housed individually in metabolic cages and urine was collected over a 24-h period. Urinalysis was conducted using services provided by the University of Toledo Medical Center. The pyrogallol based QuanTtest Red Total Protein Assay from Quantimetrix (Redondo Beach, CA, USA) was used to determine protein concentrations of the urine samples. A VERSAmax microplate reader from Molecular Devices (Sunnyvale, CA, USA) was used to determine absorbance at 600 nm. Protein concentrations were determined by reading against the absorbance of the QuanTtest human protein standards (25–200 mg/dL). UPE data is presented as mg/mg creatinine over a 24-h period.

STATISTICAL ANALYSES

All phenotypic data obtained from the two groups (congenic and S rats) were statistically analyzed by Student t-test. A p-value of <0.05 was considered statistically significant. Statistical analyses of the microarray data were performed with robust multiarray averaging and Benjamini and Hochberg adjustment using the R statistical package (version 2.8.1).

RESULTS

The rat strains chosen as tools for this study were the Dahl S rat and $a > 99\%$ genetically identical strain, the S.LEW congenic strain, which has $a < 330$ kb of the LEW rat genome introgressed onto the genome of the S rat (**Figure 1A**). At 52 days of age, the systolic blood pressure of the congenic strain measured by the telemetry method was 138 ± 2 mmHg compared with that of the S, 132 ± 2 mmHg, $p < 0.01$ (Gopalakrishnan et al., 2011). The introgressed segment contained the gene rififylin, overexpression of which is known to cause a delay in endosomal recycling in cardiomyocytes (Gopalakrishnan et al., 2011). Rififylin was also transcribed in the kidneys of both the S and the congenic strain (**Figure 1B**), however, kidneys of congenic rats had a 1.56-fold higher mRNA of rififylin compared with that of the S ($p < 0.001$; **Figure 1C**). Protein levels of rififylin were also higher both in the kidney and within the proximal tubules of congenic rats compared with S (**Figures 1D,E**).

To study the alterations in the renal transcriptome between the S and the congenic strain with increased expression of rififylin, a whole genome renal transcriptome analysis was conducted. A total of 1082 probes representing 838 genes and 244 ESTs were upregulated in the congenic strain compared with S. Similarly, a total of 785 probes representing 423 genes and 362

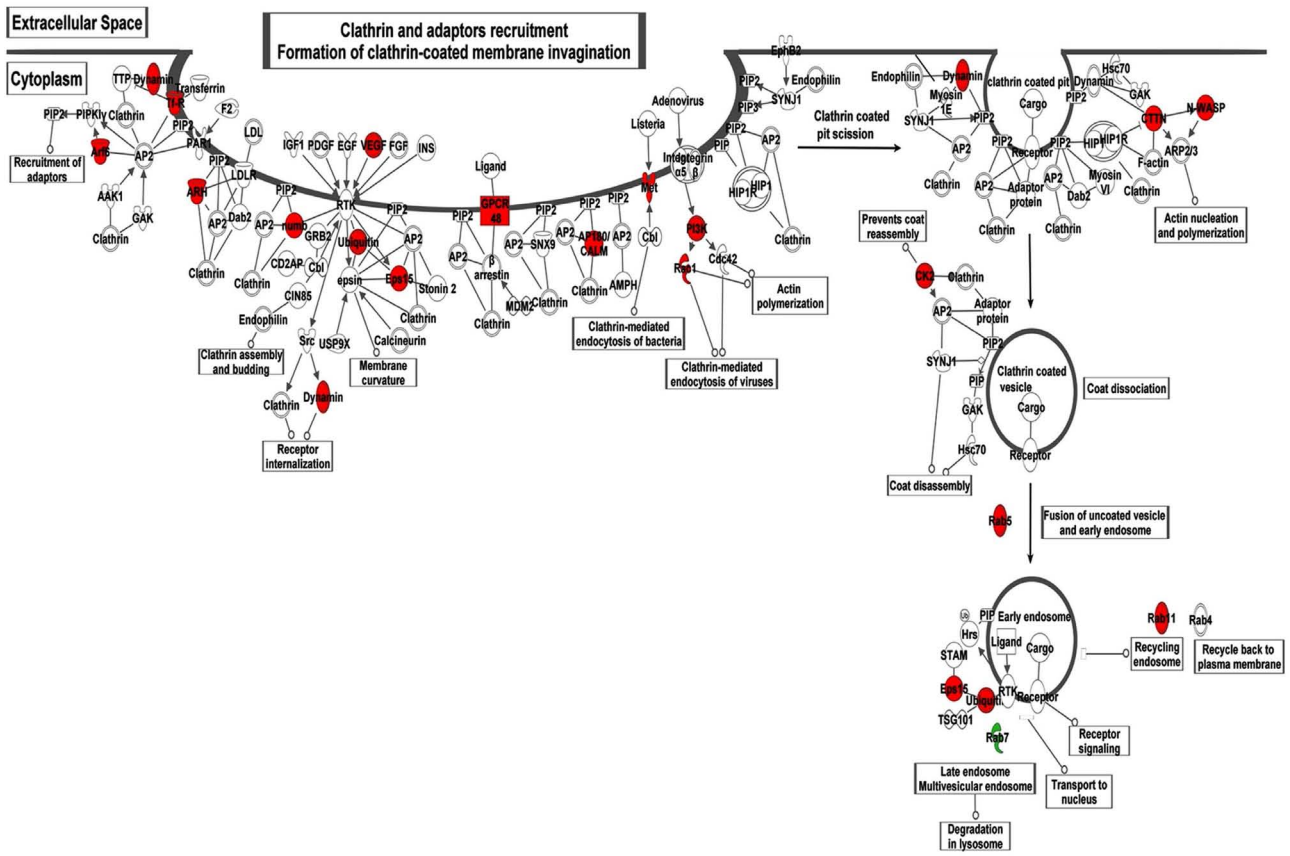

FIGURE 2 | Illustration of the IPA network analysis of the differentially expressed transcripts associated with Clathrin-mediated endocytosis and recycling. Transcripts shown in red were upregulated and green were down-regulated in the congenic strain compared with S. The fold changes of the corresponding Affymetrix probes are given in **Table 1**.

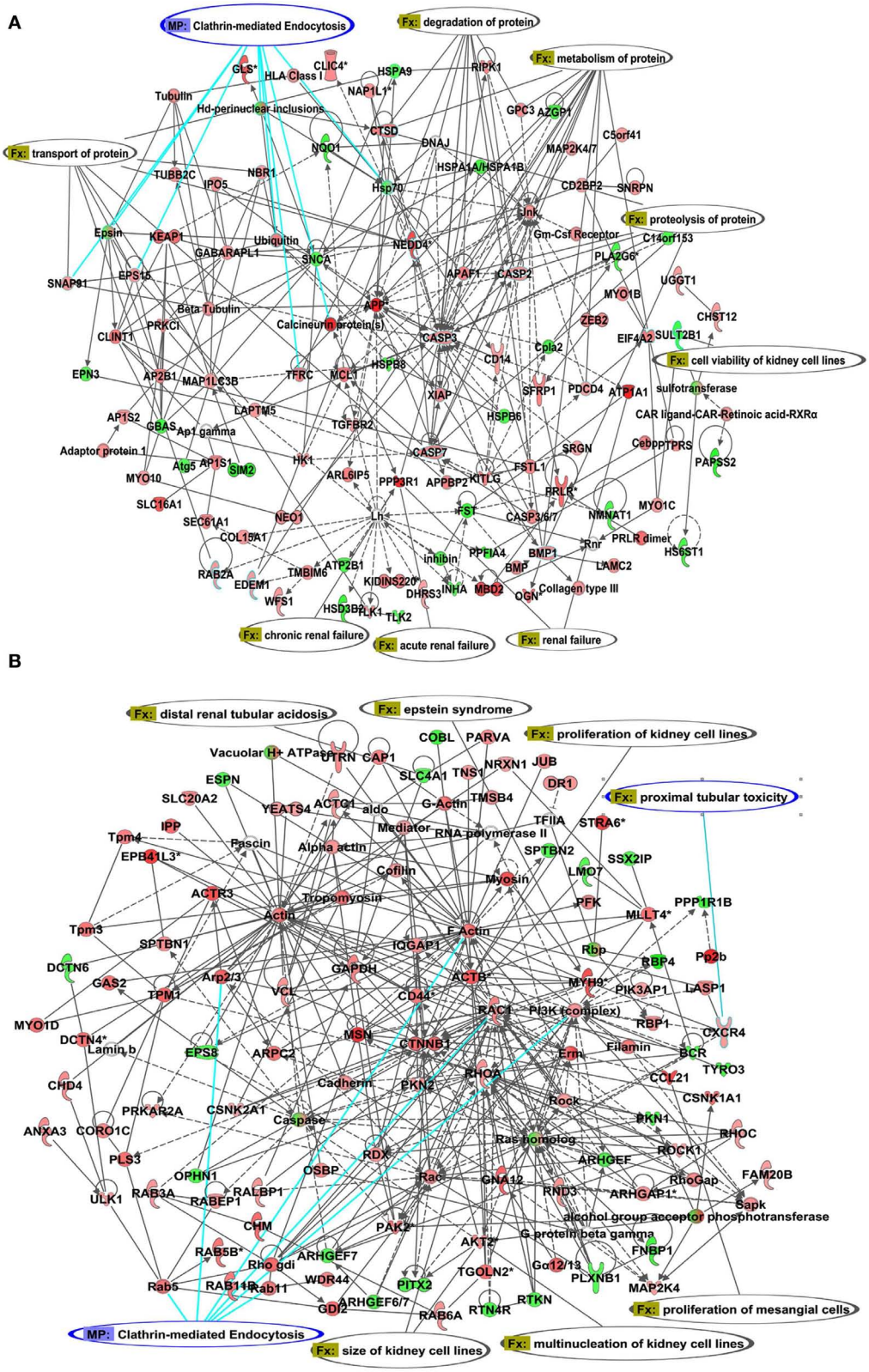

FIGURE 3 | Illustration of the IPA networks of transcripts associated with cell morphology and renal function. (A) network 1 with *Atp1a1* and **(B)** network with *Rab* proteins Transcripts shown in red were upregulated and transcripts shown in green were down-regulated in the congenic strain compared with S. The fold changes of the corresponding Affymetrix probes are given in **Table A1** in Appendix.

ESTs were down-regulated in the congenic strain compared with S (GSE30770). Among these transcripts, the highest differential expression of 5.33-fold was observed with *Atp1a1*, which was upregulated in the congenic strain compared with S (**Table A1** in Appendix). Notably, a number of transcripts coding for proteins either directly or indirectly related to the sorting of endosomes were upregulated in the congenic strain compared with S. The relative changes in gene expression of differentially expressed genes are in **Table 1**. The networks of these gene products that facilitate clathrin-coated membrane invagination and endocytosis are depicted in **Figure 2**. The other genes differentially expressed belonged to two prominent networks related to cellular morphology and renal associated function (**Figures 3A,B**). While *Atp1a1* featured in the network represented in **Figure 3A**, several transcripts coding for Rab proteins including *Rab5* which regulates transport from plasma membrane to EEs and *Rab11* involved in endocytic recycling (Trischler et al., 1999) featured in the network represented in **Figure 3B**. The fold changes of all the transcripts within these two additional networks are given in the **Table A1** in Appendix.

Next, we assessed the content of the protein product of the most differentially expressed gene, *Atp1a1*. Within the proximal tubules, the total protein content of the alpha subunit of Na^+K^+ATPase (referred to hereafter as alpha 1) was not different between S and the congenic strain (data not shown). Protein levels of alpha 1 were not different between the early endosomal fractions isolated from the proximal tubules of the congenic strain and the S (data not shown). However, surface biotinylation experiments indicated that the content of alpha 1 was notably higher on the cell membranes from the congenic strain compared with S (**Figure 4**). Total polyubiquitinated proteins were also significantly higher in the congenic strain compared with S (**Figure 5**).

To assess the extent of endosomal recycling in the kidney of the congenic strain with increased expression of *Rffl*, recycling of fluorescently labeled transferrin was monitored in individual proximal tubules. As shown in **Figures 6A,B**, recycling of transferrin was significantly delayed in the congenic strain compared with S.

These observations, coupled with the fact that rififylin residing within the congenic segment is a regulator of cellular protein recycling, suggested that the primary delay in recycling of endosomes caused membrane proteins to accumulate intracellularly within the proximal tubules from the congenic strain. Because similar defects in membrane traffic and enhanced degradation of proteins are known to cause proteinuria (Marshansky et al., 2002), we tested the urine composition of the two rat strains at a very young age of 53 days. The total protein excretion was significantly higher by 31% in the congenic strain (11.91 ± 1.12 mg/mg creatinine/day) compared to that in the S (8.26 ± 1.08 mg/mg creatinine/day, $p = 0.016$; **Figure 7**). The other urinary parameters analyzed, i.e., urea nitrogen, glucose, and creatinine excretion were not significantly different between the S and the congenic strain (data not shown).

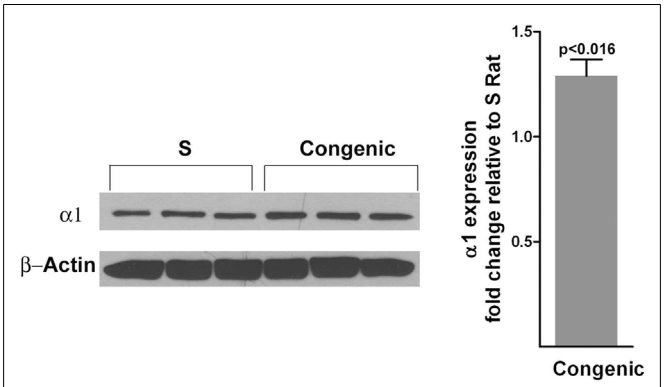

FIGURE 4 | Quantitation of the α-1 subunit of Na^+K^+ATPase on the plasma membranes of cells from proximal tubules ($n = 3$ animals per group). The surface biotinylation experiment on isolated proximal tubules was conducted as described under methods. The top panel of the western blot was probed with antibodies to the α-1 subunit of Na^+K^+ATPase. The bottom panel was probed with antibodies to β-actin. Densitometric scans are shown on the right hand side.

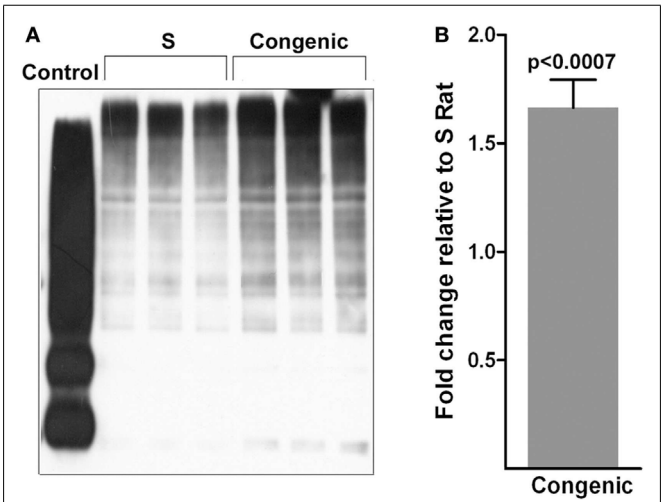

FIGURE 5 | Polyubiquitination of proteins. (A) Immunoblot of polyubiquitinated proteins in whole-cell lysates from S ($n = 3$) and congenic ($n = 3$) rat kidneys. Control is from the Pierce ubiquitination kit. **(B)** Quantification of the blot shown in **(A)** by densitometry.

DISCUSSION

Hypertension in the Dahl S rat is accompanied with proteinuria (Sustarsic et al., 1981; Sterzel et al., 1988; Garrett et al., 2003). Compared to the S rat, both blood pressure (Gopalakrishnan et al., 2011) and UPE are further increased in the congenic strain reported in the current study. We have previously demonstrated that overexpression of rififylin in the neonatal cardiomyocytes of this congenic strain is linked to short QT-interval and hypertension (Gopalakrishnan et al., 2011). While alterations in QT-interval can contribute to the development of hypertension (Baumert et al., 2011), it does not independently explain the observed increase in UPE of the congenic strain. Because rififylin is also reported to be expressed in other tissues (Coumailleau et al., 2004), we suspected that the fundamental cellular mechanism altered by the overexpression of rififylin could be operational

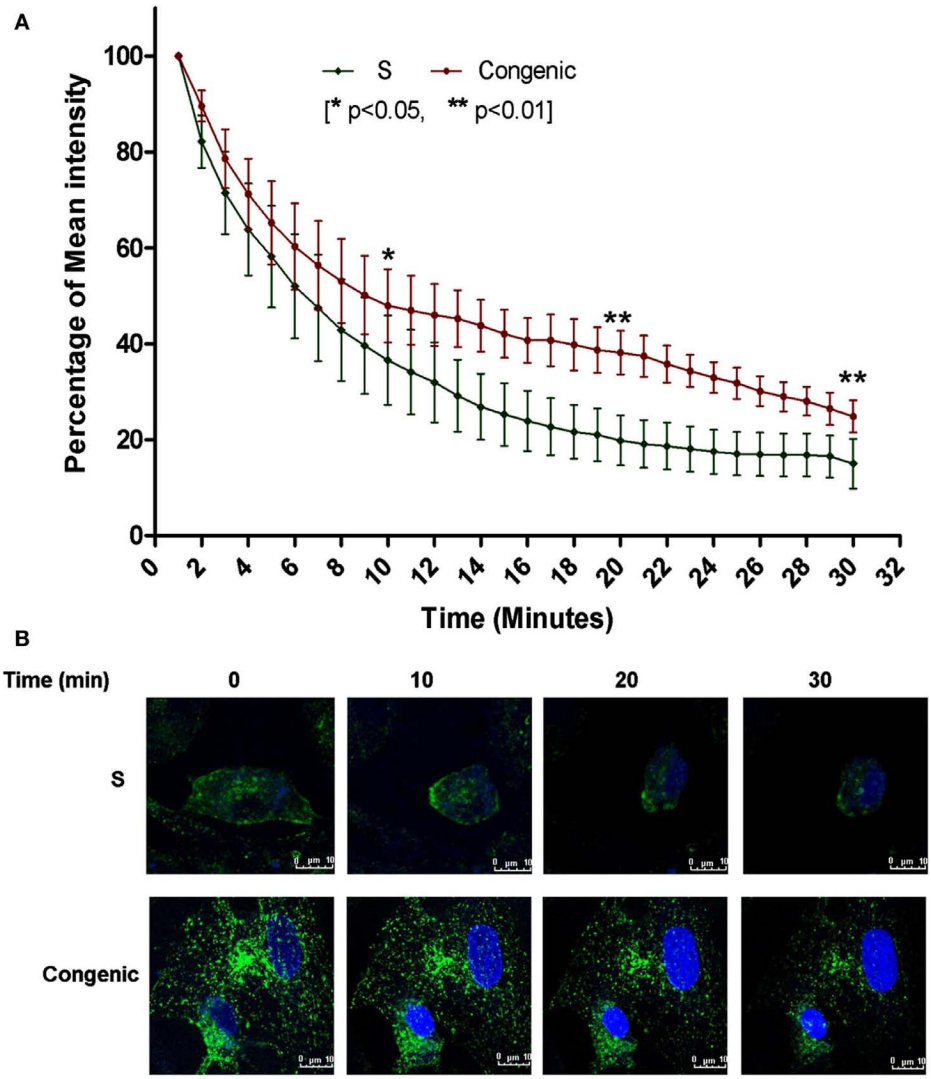

FIGURE 6 | Defective transferrin recycling in the proximal tubules from the congenic rats. (A) The disappearance of fluorescently labeled transferrin was plotted using the initial mean intensity of labeled internalized transferrin (±SEM) by the proximal tubules taken as 100% in three independent experiments ($n = 3$ animals per group) conducted in duplicates (**$p < 0.01$; *$p < 0.05$). **(B)** Representative images, green – fluorescently labeled transferring, blue – DRAQ staining of nuclei.

in the kidney wherein rififylin is expressed at higher levels in the congenic strain compared with S. The present study provides evidence to suggest that upregulation of rififylin in the congenic strain compared with S is not limited to the heart, but is also observed at least in one additional organ, the kidney. Functional analysis of rififylin revealed that endocytic recycling is delayed within the proximal tubules. The renal transcriptome signature is reminiscent of perturbations in the endosomal sorting and transport pathways, alterations in which are reported to lead to proteinuria (Nielsen, 1994; Nielsen and Christensen, 2010).

Several structural proteins and GTPase regulators are indispensable for recycling endosomes (Grant and Donaldson, 2009; Schweitzer et al., 2011). Rififylin, also known as Carp-2, is a recent addition to the growing list of proteins associated with the cellular recycling machinery. Coumailleau et al. (2004) described that overexpression of rififylin represents a novel means to inhibit recycling. Using deletion mutants, they demonstrated that the amino-terminal region of rififylin is critical for the recruitment of Rffl to recycling endocytic membranes and for the inhibition of recycling. The current study of delayed recycling in proximal tubules caused by increased renal expression of *Rffl* along with a previous similar report on cardiomyocytes from our group (Gopalakrishnan et al., 2011) represent the first two *in vivo* validations of the *in vitro* studies on HeLa cells reported by Coumailleau et al. (2004).

Transcriptome profiling demonstrates that there are numerous changes in gene transcript levels in the kidneys of S versus the congenic strain. According to the IPA network analysis, genes upregulated were in networks including cellular assembly and organization, cellular function and maintenance and cell morphology,

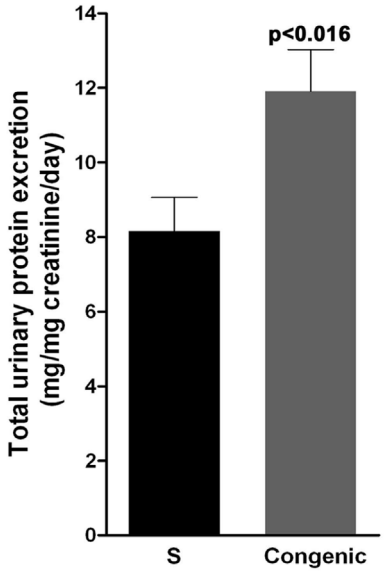

FIGURE 7 | Urinary protein excretion in S and congenic rats. Twenty-four hours urine samples were collected from S ($n = 13$) and congenic ($n = 12$) rats and total protein was quantitated. UPE data is presented as mg/mg creatinine over a 24-h period.

all of which are processes known to involve endocytic recycling (Schweitzer et al., 2011). Two lines of evidence further point to impaired endocytic recycling: (1) upregulation of transcripts in the clathrin-mediated endocytosis and recycling pathways and (2) delayed recycling of transferrin.

Additionally, Coumailleau et al. (2004) have reported that rififylin *per se* does not affect endocytosis. Therefore any alteration in endocytosis is perhaps a representation of the concerted cellular feedback response to the primary defect in recycling in order to maintain cellular homeostasis.

A defect in recycling should either demonstrate an increased accumulation of cargo within the endosomes or trigger degradation of proteins. Evidence from increased polyubiquitinated proteins within the proximal tubules of the congenic strain compared with S point to the latter, i.e., upregulation of the cellular degradation machinery. This is not surprising because rififylin is also a known E3 ubiquitin ligase and we have previously demonstrated similar increased cellular polyubiquitination of proteins within the cardiomyocytes of the congenic strain used in the current study compared with S (Gopalakrishnan et al., 2011). Increased accumulation of polyubiquitination leads to cellular stress, which is known to adversely affect proteinuria (Meyer-Schwesinger et al., 2011). Therefore, it is possible that the increased accumulation of polyubiquitinated proteins in the congenic strain relative to the S, atleast in part, contributes to the observed increased in proteinuria of the congenic strain.

The increase in blood pressure of this strain has been previously attributed partly to increased heart rate observed in the congenic strain (Gopalakrishnan et al., 2011). The current study indicates that an additional factor contributing to the increased blood pressure of the congenic strain could be due to the compensatory mechanism of increased transcription and availability of the Na^+K^+ATPase at the surface of cells within the proximal tubules, which may cause increased sodium retention and thereby increase blood pressure.

Overall, three main reasons lead us to conclude that overexpression of rififylin within the congenic strain compared with S is a contributor to the observed alterations in kidney function as noted by alterations in proteinuria – (1) the two strains compared were genetically identical except for the very short <330 kb congenic segment harboring rififylin; (2) two known functional consequences of delayed endocytic recycling and accumulation of polyubiquitinated proteins (Coumailleau et al., 2004, 2005) as a result of overexpression of rififylin were recapitulated in the congenic strain; and (3) *Rffl* is a candidate gene within the congenic interval that is reported to affect both recycling and polyubiquitination. Despite these compelling arguments, it remains to be determined using future mapping studies to further dissect the <330 kb congenic segment as to whether additional factors within the congenic interval also contribute to the reported phenotypes.

Given that alpha1 is not within the congenic segment, it is also reasonable to conclude that the primary physiological perturbations that may have lead to the observed increase in transcription of alpha1 and the increased alpha 1 content on the plasma membrane is a compensatory mechanism. Of course, we would expect increased blood pressure as one of the consequences to this compensatory mechanism and the congenic strain indeed has higher blood pressure at a very young age of 52 days. Further, a prolonged cellular stress as a result of accumulation of excess proteins marked for degradation could be viewed as being highly detrimental because the congenic strain is reported to have a decreased life span compared with S (Gopalakrishnan et al., 2011).

Genome-wide association and linkage studies in humans and model organisms point to a number of candidate genes for chronic renal disease and/or albuminuria (Liu and Freedman, 2005; Krolewski et al., 2006; Turner et al., 2006; Arar et al., 2007, 2008; Garrett et al., 2007, 2010; Hwang et al., 2007; Iyengar et al., 2007; Leon et al., 2007; Martinez et al., 2010; Sterken and Kiryluk, 2010). The genome-wide association studies in particular only represent <1.5% of the total variance in albuminuria observed in human populations. Therefore a large number of loci causing or contributing to renal function disorders in humans remain unidentified. Genome-wide studies have identified single nucleotide polymorphisms around the gene coding for rififylin in humans to QT-intervals (Newton-Cheh et al., 2009; Pfeufer et al., 2009), but not to any renal phenotypes. Through the discovery of a link between endosomal recycling, enhanced degradation, and a resultant altered trafficking of proteins within the proximal tubules, the present study provides the basis for evaluating rififylin as a novel candidate gene for renal disease characterized by proteinuria in humans.

ACKNOWLEDGMENTS

This work was supported by RO1 grants (HL020176, HL076709) to Bina Joe from the National Heart Lung and Blood Institute of the National Institutes of Health, Bethesda, USA.

REFERENCES

Arar, N., Nath, S., Thameem, F., Bauer, R., Voruganti, S., Comuzzie, A., Cole, S., Blangero, J., MacCluer, J., and Abboud, H. (2007). Genome-wide scans for microalbuminuria in Mexican Americans: the San Antonio Family Heart Study. *Genet. Med.* 9, 80–87.

Arar, N. H., Voruganti, V. S., Nath, S. D., Thameem, F., Bauer, R., Cole, S. A., Blangero, J., MacCluer, J. W., Comuzzie, A. G., and Abboud, H. E. (2008). A genome-wide search for linkage to chronic kidney disease in a community-based sample: the SAFHS. *Nephrol. Dial. Transplant.* 23, 3184–3191.

Baumert, M., Schlaich, M. P., Nalivaiko, E., Lambert, E., Sari, C. I., Kaye, D. M., Elser, M. D., Sanders, P., and Lambert, G. (2011). Relation between QT interval variability and cardiac sympathetic activity in hypertension. *Am. J. Physiol. Heart Circ. Physiol.* 300, H1412–H1417.

Brown, D., and Stow, J. L. (1996). Protein trafficking and polarity in kidney epithelium: from cell biology to physiology. *Physiol. Rev.* 76, 245–297.

Coumailleau, F., Babinet, C., and Cohen-Tannoudji, M. (2005). Inhibition of endocytic recycling by Rififylin. *Med. Sci. (Paris)* 21, 235–237.

Coumailleau, F., Das, V., Alcover, A., Raposo, G., Vandormael-Pournin, S., Le Bras, S., Baldacci, P., Dautry-Varsat, A., Babinet, C., and Cohen-Tannoudji, M. (2004). Over-expression of rififylin, a new RING finger and FYVE-like domain-containing protein, inhibits recycling from the endocytic recycling compartment. *Mol. Biol. Cell* 15, 4444–4456.

Garrett, M. R., Dene, H., and Rapp, J. P. (2003). Time-course genetic analysis of albuminuria in Dahl salt-sensitive rats on low-salt diet. *J. Am. Soc. Nephrol.* 14, 1175–1187.

Garrett, M. R., Gunning, W. T., Radecki, T., and Richard, A. (2007). Dissection of a genetic locus influencing renal function in the rat and its concordance with kidney disease loci on human chromosome 1q21. *Physiol. Genomics* 30, 322–334.

Garrett, M. R., Pezzolesi, M. G., and Korstanje, R. (2010). Integrating human and rodent data to identify the genetic factors involved in chronic kidney disease. *J. Am. Soc. Nephrol.* 21, 398–405.

Golachowska, M. R., Hoekstra, D., and van Ijzendoorn, S. C. (2010). Recycling endosomes in apical plasma membrane domain formation and epithelial cell polarity. *Trends Cell Biol.* 20, 618–626.

Gopalakrishnan, K., Morgan, E. E., Yerga-Woolwine, S., Farms, P., Kumarasamy, S., Kalinoski, A., Liu, X., Wu, J., Liu, L., and Joe, B. (2011). Augmented rififylin is a risk factor linked to aberrant cardiomyocyte function, short-QT interval and hypertension. *Hypertension* 57, 764–771.

Grant, B. D., and Donaldson, J. G. (2009). Pathways and mechanisms of endocytic recycling. *Nat. Rev. Mol. Cell Biol.* 10, 597–608.

Hryciw, D. H., Ekberg, J., Pollock, C. A., and Poronnik, P. (2006). ClC-5: a chloride channel with multiple roles in renal tubular albumin uptake. *Int. J. Biochem. Cell Biol.* 38, 1036–1042.

Hwang, S. J., Yang, Q., Meigs, J. B., Pearce, E. N., and Fox, C. S. (2007). A genome-wide association for kidney function and endocrine-related traits in the NHLBI's Framingham Heart Study. *BMC Med. Genet.* 8(Suppl. 1), S10. doi:10.1186/1471-2350-8-S1-S10

Iyengar, S. K., Abboud, H. E., Goddard, K. A., Saad, M. F., Adler, S. G., Arar, N. H., Bowden, D. W., Duggirala, R., Elston, R. C., Hanson, R. L., Ipp, E., Kao, W. H., Kimmel, P. L., Klag, M. J., Knowler, W. C., Meoni, L. A., Nelson, R. G., Nicholas, S. B., Pahl, M. V., Parekh, R. S., Quade, S. R., Rich, S. S., Rotter, J. I., Scavini, M., Schelling, J. R., Sedor, J. R., Sehgal, A. R., Shah, V. O., Smith, M. W., Taylor, K. D., Winkler, C. A., Zager, P. G., and Freedman, B. I. (2007). Genome-wide scans for diabetic nephropathy and albuminuria in multiethnic populations: the family investigation of nephropathy and diabetes (FIND). *Diabetes* 56, 1577–1585.

Krolewski, A. S., Poznik, G. D., Placha, G., Canani, L., Dunn, J., Walker, W., Smiles, A., Krolewski, B., Fogarty, D. G., Moczulski, D., Araki, S., Makita, Y., Ng, D. P., Rogus, J., Duggirala, R., Rich, S. S., and Warram, J. H. (2006). A genome-wide linkage scan for genes controlling variation in urinary albumin excretion in type II diabetes. *Kidney Int.* 69, 129–136.

Kumarasamy, S., Gopalakrishnan, K., Toland, E. J., Yerga-Woolwine, S., Farms, P., Morgan, E. E., and Joe, B. (2011). Refined mapping of blood pressure quantitative trait loci using congenic strains developed from two genetically hypertensive rat models. *Hypertens. Res.* 34, 1263–1270.

Leon, J. M., Freedman, B. I., Miller, M. B., North, K. E., Hunt, S. C., Eckfeldt, J. H., Lewis, C. E., Kraja, A. T., Djousse, L., and Arnett, D. K. (2007). Genome scan of glomerular filtration rate and albuminuria: the HyperGEN study. *Nephrol. Dial. Transplant.* 22, 763–771.

Liu, J., Kesiry, R., Periyasamy, S. M., Malhotra, D., Xie, Z., and Shapiro, J. I. (2004). Ouabain induces endocytosis of plasmalemmal Na/K-ATPase in LLC-PK1 cells by a clathrin-dependent mechanism. *Kidney Int.* 66, 227–241.

Liu, J., Periyasamy, S. M., Gunning, W., Fedorova, O. V., Bagrov, A. Y., Malhotra, D., Xie, Z., and Shapiro, J. I. (2002). Effects of cardiac glycosides on sodium pump expression and function in LLC-PK1 and MDCK cells. *Kidney Int.* 62, 2118–2125.

Liu, J., Yan, Y., Liu, L., Xie, Z., Malhotra, D., Joe, B., and Shapiro, J. I. (2011). Impairment of Na/K-ATPase signaling in renal proximal tubule contributes to Dahl salt-sensitive hypertension. *J. Biol. Chem.* 286, 22806–22813.

Liu, Y., and Freedman, B. I. (2005). Genetics of progressive renal failure in diabetic kidney disease. *Kidney Int. Suppl.* 99, S94–S97.

Livak, K. J., and Schmittgen, T. D. (2001). Analysis of relative gene expression data using real-time quantitative PCR and the 2(-Delta Delta C(T)) method. *Methods* 25, 402–408.

Marshansky, V., Ausiello, D. A., and Brown, D. (2002). Physiological importance of endosomal acidification: potential role in proximal tubulopathies. *Curr. Opin. Nephrol. Hypertens.* 11, 527–537.

Martinez, F., Mansego, M. L., Chaves, F. J., and Redon, J. (2010). Genetic bases of urinary albumin excretion and related traits in hypertension. *J. Hypertens.* 28, 213–225.

Maxfield, F. R., and McGraw, T. E. (2004). Endocytic recycling. *Nat. Rev. Mol. Cell Biol.* 5, 121–132.

Meyer-Schwesinger, C., Meyer, T. N., Sievert, H., Hoxha, E., Sachs, M., Klupp, E. M., Munster, S., Balabanov, S., Carrier, L., Helmchen, U., Thaiss, F., and Stahl, R. A. (2011). Ubiquitin C-terminal hydrolase-l1 activity induces polyubiquitin accumulation in podocytes and increases proteinuria in rat membranous nephropathy. *Am. J. Pathol.* 178, 2044–2057.

Newton-Cheh, C., Eijgelsheim, M., Rice, K. M., de Bakker, P. I., Yin, X., Estrada, K., Bis, J. C., Marciante, K., Rivadeneira, F., Noseworthy, P. A., Sotoodehnia, N., Smith, N. L., Rotter, J. I., Kors, J. A., Witteman, J. C., Hofman, A., Heckbert, S. R., O'Donnell, C. J., Uitterlinden, A. G., Psaty, B. M., Lumley, T., Larson, M. G., and Stricker, B. H. (2009). Common variants at ten loci influence QT interval duration in the QTGEN Study. *Nat. Genet.* 41, 399–406.

Nielsen, R., and Christensen, E. I. (2010). Proteinuria and events beyond the slit. *Pediatr. Nephrol.* 25, 813–822.

Nielsen, S. (1993). Endocytosis in proximal tubule cells involves a two-phase membrane-recycling pathway. *Am. J. Physiol.* 264, C823–C835.

Nielsen, S. (1994). Endocytosis in renal proximal tubules. Experimental electron microscopical studies of protein absorption and membrane traffic in isolated, in vitro perfused proximal tubules. *Dan. Med. Bull.* 41, 243–263.

Pfeufer, A., Sanna, S., Arking, D. E., Muller, M., Gateva, V., Fuchsberger, C., Ehret, G. B., Orru, M., Pattaro, C., Kottgen, A., Perz, S., Usala, G., Barbalic, M., Li, M., Putz, B., Scuteri, A., Prineas, R. J., Sinner, M. F., Gieger, C., Najjar, S. S., Kao, W. H., Muhleisen, T. W., Dei, M., Happle, C., Mohlenkamp, S., Crisponi, L., Erbel, R., Jockel, K. H., Naitza, S., Steinbeck, G., Marroni, F., Hicks, A. A., Lakatta, E., Muller-Myhsok, B., Pramstaller, P. P., Wichmann, H. E., Schlessinger, D., Boerwinkle, E., Meitinger, T., Uda, M., Coresh, J., Kaab, S., Abecasis, G. R., and Chakravarti, A. (2009). Common variants at ten loci modulate the QT interval duration in the QTSCD Study. *Nat. Genet.* 41, 407–414.

Schweitzer, J. K., Sedgwick, A. E., and D'Souza-Schorey, C. (2011). ARF6-mediated endocytic recycling impacts cell movement, cell division and lipid homeostasis. *Semin. Cell Dev. Biol.* 22, 39–47.

Steinman, R. M., Mellman, I. S., Muller, W. A., and Cohn, Z. A. (1983). Endocytosis and the recycling of plasma membrane. *J. Cell Biol.* 96, 1–27.

Stendel, C., Roos, A., Kleine, H., Arnaud, E., Ozcelik, M., Sidiropoulos, P. N., Zenker, J., Schupfer, F., Lehmann, U., Sobota, R. M., Litchfield, D. W., Luscher, B., Chrast, R., Suter, U., and Senderek, J. (2010). SH3TC2, a protein mutant in Charcot-Marie-Tooth neuropathy, links peripheral nerve myelination to endosomal recycling. *Brain* 133, 2462–2474.

Sterken, R., and Kiryluk, K. (2010). The genetics of albuminuria: from haplotype association mapping in mice to genetic causation in humans. *Kidney Int.* 77, 173–175.

Sterzel, R. B., Luft, F. C., Gao, Y., Schnermann, J., Briggs, J. P., Ganten, D., Waldherr, R., Schnabel, E., and Kriz, W. (1988). Renal disease and the development of hypertension in salt-sensitive Dahl rats. *Kidney Int.* 33, 1119–1129.

Sustarsic, D. L., McPartland, R. P., and Rapp, J. P. (1981). Developmental patterns of blood pressure and urinary protein, kallikrein, and prostaglandin E2 in Dahl salt-hypertension-susceptible rats. *J. Lab. Clin. Med.* 98, 599–606.

Trischler, M., Stoorvogel, W., and Ullrich, O. (1999). Biochemical analysis of distinct Rab5- and Rab11-positive endosomes along the transferrin pathway. *J. Cell Sci.* 112, 4773–4783.

Turner, S. T., Kardia, S. L., Mosley, T. H., Rule, A. D., Boerwinkle, E., and de Andrade, M. (2006). Influence of genomic loci on measures of chronic kidney disease in hypertensive sibships. *J. Am. Soc. Nephrol.* 17, 2048–2055.

Yamamoto, K., Cox, J. P., Friedrich, T., Christie, P. T., Bald, M., Houtman, P. N., Lapsley, M. J., Patzer, L., Tsimaratos, M., Van, T. H. W. G., Yamaoka, K., Jentsch, T. J., and Thakker, R. V. (2000). Characterization of renal chloride channel (CLCN5) mutations in Dent's disease. *J. Am. Soc. Nephrol.* 11, 1460–1468.

Conflict of Interest Statement: The authors declare that the research was conducted in the absence of any commercial or financial relationships that could be construed as a potential conflict of interest.

Received: 02 June 2012; accepted: 11 July 2012; published online: 08 August 2012.
Citation: Gopalakrishnan K, Kumarasamy S, Yan Y, Liu J, Kalinoski A, Kothandapani A, Farms P and Joe B (2012) Increased expression of rififfylin in a < 330 kb congenic strain is linked to impaired endosomal recycling in proximal tubules. Front. Gene. ***3****:138. doi: 10.3389/fgene.2012.00138*
This article was submitted to Frontiers in Genomic Physiology, a specialty of Frontiers in Genetics.

APPENDIX

Table A1 | Differentially expressed transcripts in networks (Figures 3A,B).

Affymetrix ID	Fold change	*p*-Value	Symbol	Entrez gene name
1371108_a_at	5.3380	0.0334	*Atp1a1*	ATPase, Na^+/K^+ transporting, alpha 1 polypeptide
1380533_at	4.2845	0.0180	*App*	Amyloid beta (A4) precursor protein
1369152_at	3.3827	0.0319	*Ppp3r1*	Protein phosphatase 3, regulatory subunit B, alpha
1368948_at	3.1624	0.0383	*Msn*	Moesin
1370503_s_at	2.9373	0.0422	*Epb41l3*	Erythrocyte membrane protein band 4.1-like 3
1390525_a_at	2.7414	0.0397	*Stra6*	Stimulated by retinoic acid gene 6 homolog (mouse)
1378015_at	2.6839	0.0206	*Ccl21*	Chemokine (C–C motif) ligand 21
1388774_at	2.6075	0.0051	*Mbd2*	Methyl-cpg binding domain protein 2
1383899_at	2.5886	0.0335	*Nedd4*	Neural precursor cell expressed, developmentally down-regulated 4
1395886_at	2.5617	0.0327	*Actr3*	ARP3 actin-related protein 3 homolog (yeast)
1387402_at	2.5213	0.0303	*Myh9*	Myosin, heavy chain 9, non-muscle
AFFX_Rat_beta-actin_5_at	2.4164	0.0236	*Actb*	Actin, beta
1386981_at	2.4077	0.0157	*Slc16a1*	Solute carrier family 16, member 1 (monocarboxylic acid transporter 1)
1382616_at	2.3050	0.0359	*Gls*	Glutaminase
1369733_at	2.2009	0.0258	*Ctnnb1*	Catenin (cadherin-associated protein), beta 1, 88 kDa
1370288_a_at	2.1568	0.0201	*Tpm1*	Tropomyosin 1 (alpha)
1369278_at	2.1499	0.0202	*Gna12*	Guanine nucleotide binding protein (G protein) alpha 12
1398822_at	2.0847	0.0284	*Gdi2*	GDP dissociation inhibitor 2
1369227_at	2.0708	0.0137	*Chm*	Choroideremia (Rab escort protein 1)
1392406_at	2.0290	0.0370	*Ipp*	Intracisternal A particle-promoted polypeptide
1370789_a_at	2.0256	0.0435	*Prlr*	Prolactin receptor
1369312_a_at	2.0143	0.0280	*Csnk1a1*	Casein kinase 1, alpha 1
1371028_at	2.0125	0.0372	*Tgoln2*	Trans-golgi network protein 2
1371139_at	2.0094	0.0475	*Pls3*	Plastin 3
1387810_at	2.0016	0.0177	*Keap1*	Kelch-like ECH-associated protein 1
1396267_at	1.9907	0.0392	*Pak2*	p21 protein (Cdc42/Rac)-activated kinase 2
1368537_at	1.9863	0.0225	*Dctn4*	Dynactin 4 (p62)
1383263_at	1.9628	0.0177	*Ogn*	Osteoglycin
1387392_at	1.9581	0.0276	*Mllt4*	Myeloid/lymphoid or mixed-lineage leukemia; translocated to, 4
1369779_at	1.9506	0.0099	*Myo1d*	Myosin ID
1375137_at	1.9173	0.0366	*Arpc2*	Actin-related protein 2/3 complex, subunit 2, 34 kDa
1379452_at	1.9090	0.0372	*Gas2*	Growth arrest-specific 2
1371239_s_at	1.9033	0.0379	*Tpm3*	Tropomyosin 3, gamma
1393288_at	1.8966	0.0366	*Rab5b*	RAB5B, member RAS oncogene family
1370141_at	1.8715	0.0280	*Mcl1*	Myeloid cell leukemia sequence 1 (BCL2-related)
1394965_at	1.8507	0.0450	*Clint1*	Clathrin interactor 1
1387952_a_at	1.8175	0.0221	*Cd44*	CD44 molecule (Indian blood group)
1398825_at	1.8017	0.0434	*Rab11b*	RAB11B, member RAS oncogene family
1397697_at	1.7912	0.0321	*Eif4a2*	Eukaryotic translation initiation factor 4A2
1371113_a_at	1.7874	0.0411	*Tfrc*	Transferrin receptor (p90, CD71)
1367651_at	1.7835	0.0464	*Ctsd*	Cathepsin D
1398311_a_at	1.7425	0.0411	*Kidins220*	Kinase d-interacting substrate, 220 kDa
1369197_at	1.7379	0.0268	*Apaf1*	Apoptotic peptidase activating factor 1
1368808_at	1.7327	0.0282	*Cap1*	CAP, adenylate cyclase-associated protein 1 (yeast)
1368838_at	1.7273	0.0388	*Tpm4*	Tropomyosin 4
1396214_at	1.7272	0.0205	*Kitlg*	KIT ligand
1369319_at	1.7265	0.0333	*Arl6ip5*	ADP-ribosylation-like factor 6 interacting protein 5
1388251_at	1.7156	0.0368	*Prkci*	Protein kinase C, iota
1396072_at	1.6782	0.0364	*Appbp2*	Amyloid beta precursor protein (cytoplasmic tail) binding protein 2
1382878_at	1.6562	0.0224	*Sfrp1*	Secreted frizzled-related protein 1

(Continued)

Table A1 | Continued

Affymetrix ID	Fold change	*p*-Value	Symbol	Entrez gene name
1391543_at	1.6489	0.0266	*Ripk1*	Receptor (TNFRSF)-interacting serine-threonine kinase 1
1382615_at	1.6466	0.0460	*Sec61a1*	Sec61 alpha 1 subunit (*S. cerevisiae*)
1397843_at	1.6417	0.0473	*Wdr44*	WD repeat domain 44
1370662_a_at	1.6351	0.0421	*Ap2b1*	Adaptor-related protein complex 2, beta 1 subunit
1369720_at	1.6345	0.0257	*Myo1b*	Myosin IB
1377769_at	1.6329	0.0402	*Ap1s1*	Adaptor-related protein complex 1, sigma 1 subunit
1372513_at	1.6297	0.0268	*Rac1*	Ras-related C3 botulinum toxin substrate 1
1387844_at	1.6240	0.0175	*Lasp1*	LIM and SH3 protein 1
1396250_at	1.6206	0.0311	*Coro1c*	Coronin, actin binding protein, 1C
1368832_at	1.6121	0.0337	*Akt2*	v-akt murine thymoma viral oncogene homolog 2
1369557_at	1.6047	0.0093	*Casp7*	Caspase 7, apoptosis-related cysteine peptidase
1393795_at	1.5994	0.0392	*Zeb2*	Zinc finger E-box binding homeobox 2
1368821_at	1.5950	0.0180	*Fstl1*	Follistatin-like 1
1383827_at	1.5947	0.0439	*Tlk1*	Tousled-like kinase 1
1378816_a_at	1.5832	0.0221	*osbp*	Oxysterol binding protein
1369234_at	1.5818	0.0282	*Slc20a2*	Solute carrier family 20 (phosphate transporter), member 2
1368395_at	1.5704	0.0307	*Gpc3*	Glypican 3
1388230_at	1.5600	0.0327	*Jub*	Jub, ajuba homolog (*Xenopus laevis*)
1370266_at	1.5554	0.0327	*Parva*	Parvin, alpha
1395132_at	1.5543	0.0221	*Utrn*	Utrophin
1367974_at	1.5493	0.0342	*Anxa3*	Annexin A3
1387420_at	1.5445	0.0202	*Clic4*	Chloride intracellular channel 4
1387690_at	1.5417	0.0180	*Casp3*	Caspase 3, apoptosis-related cysteine peptidase
1397200_at	1.5319	0.0277	*Chd4*	Chromodomain helicase DNA binding protein 4
1390706_at	1.5289	0.0323	*Sptbn1*	Spectrin, beta, non-erythrocytic 1
AFFX_Rat_Hexokinase_3_at	1.5278	0.0388	*Hk1*	Hexokinase 1
1370599_a_at	1.5255	0.0292	*Ptprs*	Protein tyrosine phosphatase, receptor type, S
1388762_at	1.5226	0.0374	*Iqgap1*	IQ motif containing GTPase activating protein 1
1369248_a_at	1.5212	0.0442	*Xiap*	X-linked inhibitor of apoptosis
1367939_at	1.5168	0.0362	*Rbp1*	Retinol binding protein 1, cellular
1384938_at	1.5126	0.0470	*Arhgap1*	Rho GTPase activating protein 1
1369879_a_at	1.4963	0.0208	*Tmbim6*	Transmembrane BAX inhibitor motif containing 6
1378287_at	1.4835	0.0421	*Rdx*	Radixin
1371127_at	1.4768	0.0137	*Bmp1*	Bone morphogenetic protein 1
1371056_at	1.4595	0.0335	*Neo1*	Neogenin 1
1378842_at	1.4550	0.0465	*Gabarapl1*	GABA(A) receptor-associated protein like 1
1379889_at	1.4488	0.0321	*Lamc2*	Laminin, gamma 2
1367891_a_at	1.4455	0.0175	*Casp2*	Caspase 2, apoptosis-related cysteine peptidase
1396742_at	1.4423	0.0137	*Ipo5*	Importin 5
1388557_at	1.4420	0.0404	*Tubb2c*	Tubulin, beta 2C
1367981_at	1.4338	0.0436	*Rabep1*	Rabaptin, RAB GTPase binding effector protein 1
1393055_at	1.4328	0.0399	*Pkn2*	Protein kinase N2
1369085_s_at	1.4298	0.0323	*Snrpn*	Small nuclear ribonucleoprotein polypeptide N
1371103_at	1.4287	0.0268	*Rab6a*	RAB6A, member RAS oncogene family
1384005_at	1.4212	0.0355	*Dr1*	Down-regulator of transcription 1, TBP-binding (negative cofactor 2)
1394077_at	1.4202	0.0337	*Rnd3*	Rho family GTPase 3
1370130_at	1.4201	0.0393	*Rhoa*	Ras homolog gene family, member A
1379345_at	1.4034	0.0457	*Col15a1*	Collagen, type XV, alpha 1
1373473_a_at	1.3975	0.0307	*Nap1l1*	Nucleosome assembly protein 1-like 1
1375538_at	1.3927	0.0399	*Vcl*	Vinculin
1384187_at	1.3826	0.0287	*Ap1s2*	Adaptor-related protein complex 1, sigma 2 subunit
1369816_at	1.3815	0.0369	*Rab3a*	RAB3A, member RAS oncogene family

(Continued)

Table A1 | Continued

Affymetrix ID	Fold change	*p*-Value	Symbol	Entrez gene name
1368218_at	1.3797	0.0424	*Ralbp1*	ralA binding protein 1
1395548_at	1.3777	0.0331	*Eps15*	Epidermal growth factor receptor pathway substrate 15
1385797_at	1.3757	0.0377	*Actc1*	Actin, alpha, cardiac muscle 1
1382402_at	1.3687	0.0321	*Ulk1*	Unc-51-like kinase 1 (*C. elegans*)
1371059_at	1.3669	0.0302	*Prkar2a*	Protein kinase, cAMP-dependent, regulatory, type II, alpha
1383531_at	1.3571	0.0342	*C5orf41*	Chromosome 5 open reading frame 41
1381509_at	1.3482	0.0341	*Nbr1*	Neighbor of BRCA1 gene 1
1383701_at	1.3470	0.0434	*Map2k4*	Mitogen-activated protein kinase kinase 4
1373865_at	1.3468	0.0436	*Snap91*	Synaptosomal-associated protein, 91 kda homolog (mouse)
1382199_at	1.3447	0.0327	*Map1lc3b*	Microtubule-associated protein 1 light chain 3 beta
1387356_at	1.3411	0.0333	*Wfs1*	Wolfram syndrome 1 (wolframin)
1369653_at	1.3385	0.0373	*Tgfbr2*	Transforming growth factor, beta receptor II (70/80 kDa)
1371659_at	1.3332	0.0472	*Rhoc*	Ras homolog gene family, member C
1391390_at	1.3288	0.0236	*Tns1*	Tensin 1
1368006_at	1.3273	0.0236	*Laptm5*	Lysosomal protein transmembrane 5
1387654_at	1.3194	0.0428	*Myo1c*	Myosin IC
1393639_at	1.3177	0.0441	*Myo10*	Myosin X
1370097_a_at	1.3168	0.0374	*Cxcr4*	Chemokine (C-X-C motif) receptor 4
1395782_at	1.3153	0.0421	*Yeats4*	YEATS domain containing 4
1384186_at	1.3133	0.0334	*Edem1*	ER degradation enhancer, mannosidase alpha-like 1
1370087_at	1.3130	0.0327	*Rab2a*	RAB2A, member RAS oncogene family
1368953_at	1.3126	0.0437	*Uggt1*	UDP-glucose glycoprotein glucosyltransferase 1
1368490_at	1.3119	0.0212	*Cd14*	CD14 molecule
1392174_at	1.2989	0.0270	*Chst12*	Carbohydrate (chondroitin 4) sulfotransferase 12
1368932_at	1.2889	0.0411	*Rock1*	Rho-associated, coiled-coil containing protein kinase 1
1387521_at	1.2804	0.0470	*Pdcd4*	Programmed cell death 4 (neoplastic transformation inhibitor)
1380993_at	1.2497	0.0412	*Fam20b*	Family with sequence similarity 20, member B
1368655_at	1.2456	0.0321	*Srgn*	Serglycin
1387170_at	1.2384	0.0473	*Csnk2a1*	Casein kinase 2, alpha 1 polypeptide
1369404_a_at	1.2274	0.0415	*Nrxn1*	Neurexin 1
1373240_at	1.2135	0.0381	*Dhrs3*	Dehydrogenase/reductase (SDR family) member 3
1376795_at	1.2133	0.0406	*Pik3ap1*	Phosphoinositide-3-kinase adaptor protein 1
1385676_at	1.2077	0.0434	*Cd2bp2*	CD2 (cytoplasmic tail) binding protein 2
1371762_at	−3.6666	0.0137	*Rbp4*	Retinol binding protein 4, plasma
1376047_at	−1.6495	0.0180	*Papss2*	3′-phosphoadenosine 5′-phosphosulfate synthase 2
1385722_at	−1.6489	0.0369	*Sim2*	Single-minded homolog 2 (*Drosophila*)
1387843_at	−1.5384	0.0180	*Fst*	Follistatin
1368578_at	−1.4838	0.0370	*Hsd3b2*	Hydroxy-delta-5-steroid dehydrogenase, 3 beta- and steroid delta-isomerase 2
1372208_at	−1.4789	0.0333	*Ppp1r1b*	Protein phosphatase 1, regulatory (inhibitor) subunit 1B
1378632_at	−1.4769	0.0303	*Ppfia4*	Protein tyrosine phosphatase, receptor type, interacting protein, alpha 4
1384834_at	−1.4525	0.0321	*Cobl*	Cordon-bleu homolog (mouse)
1376175_at	−1.4394	0.0371	*Gbas*	Glioblastoma amplified sequence
1387599_a_at	−1.4347	0.0175	*Nqo1*	NAD(P)H dehydrogenase, quinone 1
1388721_at	−1.4340	0.0306	*Hspb8*	Heat shock 22 kDa protein 8
1377342_s_at	−1.4313	0.0333	*Fnbp1*	Formin binding protein 1
1376248_at	−1.4056	0.0402	*Sult2b1*	Sulfotransferase family, cytosolic, 2B, member 1
1368247_at	−1.3986	0.0335	*Hspa1a/hspa1b*	Heat shock 70 kDa protein 1A
1378069_at	−1.3825	0.0259	*Pkn1*	Protein kinase N1
1387234_at	−1.3696	0.0321	*Azgp1*	Alpha-2-glycoprotein 1, zinc-binding
1370385_at	−1.3498	0.0268	*Pla2g6*	Phospholipase A2, group VI (cytosolic, calcium-independent)
1388972_at	−1.3494	0.0215	*Rtn4r*	Reticulon 4 receptor
1367953_at	−1.3473	0.0492	*Tyro3*	TYRO3 protein tyrosine kinase

(Continued)

Table A1 | Continued

Affymetrix ID	Fold change	*p*-Value	Symbol	Entrez gene name
1372467_at	−1.3411	0.0425	*Hs6st1*	Heparan sulfate 6-*O*-sulfotransferase 1
1387898_at	−1.3285	0.0234	*Hspb6*	Heat shock protein, alpha-crystallin-related, B6
1397224_at	−1.3272	0.0287	*Atp2b1*	ATPase, Ca++ transporting, plasma membrane 1
1395499_at	−1.3089	0.0335	*Eps8*	Epidermal growth factor receptor pathway substrate 8
1372265_at	−1.3030	0.0459	*C14orf153*	Chromosome 14 open reading frame 153
1373494_at	−1.2980	0.0259	*Bcr*	Breakpoint cluster region
1379413_at	−1.2966	0.0378	*Nmnat1*	Nicotinamide nucleotide adenylyltransferase 1
1367812_at	−1.2966	0.0334	*Sptbn2*	Spectrin, beta, non-erythrocytic 2
1378198_at	−1.2959	0.0333	*Ophn1*	Oligophrenin 1
1367977_at	−1.2942	0.0406	*Snca*	Synuclein, alpha (non-A4 component of amyloid precursor)
1368774_a_at	−1.2666	0.0399	*Espn*	Espin
1372638_at	−1.2656	0.0434	*Arhgef7*	Rho guanine nucleotide exchange factor (GEF) 7
1368785_a_at	−1.2595	0.0406	*Pitx2*	Paired-like homeodomain 2
1382055_at	−1.2588	0.0316	*Rtkn*	Rhotekin
1387124_at	−1.2526	0.0499	*Inha*	Inhibin, alpha
1376041_at	−1.2509	0.0321	*Epn3*	Epsin 3
1396392_at	−1.2474	0.0446	*Dctn6*	Dynactin 6
1384319_at	−1.2451	0.0436	*Tlk2*	Tousled-like kinase 2
1373146_at	−1.2379	0.0323	*Ssx2ip*	Synovial sarcoma, X breakpoint 2 interacting protein
1374444_at	−1.2367	0.0424	*Plxnb1*	Plexin B1
1391915_at	−1.2313	0.0411	*Hspa9*	Heat shock 70 kDa protein 9 (mortalin)
1385526_at	−1.2223	0.0441	*Atg5*	ATG5 autophagy related 5 homolog (*S. cerevisiae*)
1381190_at	−1.2181	0.0444	*Lmo7*	LIM domain 7
1387656_at	−1.2131	0.0463	*Slc4a1*	Solute carrier family 4, anion exchanger, member 1

Statistical analyses of the microarray data were performed with RMA, robust multiarray averaging; BH, Benjamini and Hochberg adjustment using the R statistical package (version 2.8.1). The complete microarray data is available to the reviewers at the following link: http://www.ncbi.nlm.nih.gov/geo/query/acc.cgi?token=hryjdweamuioidi&acc=GSE30770